J. Korean Soc. Ind. Appl. Math. Vol.23, No.2, 93–114, 2019 http://doi.org/10.12941/jksiam.2019.23.093

AN ENERGY-STABLE AND SECOND-ORDER ACCURATE METHOD FOR SOLVING THE INCOMPRESSIBLE NAVIER-STOKES EQUATIONS

JEONGHO KIM[1], JINWOOK JUNG[1], YESOM PARK[2], CHOHONG MIN[2], AND BYUNGJOON LEE[3†]

[1]DEPARTMENT OF MATHEMATICAL SCIENCES, SEOUL NATIONAL UNIVERSITY, SOUTH KOREA

[2]DEPARTMENT OF MATHEMATICS, EWHA WOMANS UNIVERSITY, SOUTH KOREA

[3]DEPARTMENT OF MATHEMATICS, THE CATHOLIC UNIVERSITY OF KOREA, SOUTH KOREA
E-mail address: blee@catholic.ac.kr

ABSTRACT. In this article, we introduce a finite difference method for solving the Navier-Stokes equations in rectangular domains. The method is proved to be energy stable and shown to be second-order accurate in several benchmark problems. Due to the guaranteed stability and the second order accuracy, the method can be a reliable tool in real-time simulations and physics-based animations with very dynamic fluid motion.

We first discuss a simple convection equation, on which many standard explicit methods fail to be energy stable. Our method is an implicit Runge-Kutta method that preserves the energy for inviscid fluid and does not increase the energy for viscous fluid. Integration-by-parts in space is essential to achieve the energy stability, and we could achieve the integration-by-parts in discrete level by using the Marker-And-Cell configuration and central finite differences.

The method, which is implicit and second-order accurate, extends our previous method [1] that was explicit and first- order accurate. It satisfies the energy stability and assumes rectangular domains. We acknowledge that the assumption on domains is restrictive, but the method is one of the few methods that are fully stable and second-order accurate.

1. INTRODUCTION

Fluid flow is one of the fundamental phenomena in nature, and it affects our everyday lives in a ubiquitous way. The incompressible Navier-Stokes equations are essential means to understand fluid phenomena. The equations have been intensely studied, however the existence problem of their global solution is still unresolved and listed in Millennium problems [2]. Precisely speaking, the convergence of a numerical solution may not be proper, for the global solution is unknown. Customarily, the order of accuracy refers to the approximation order of the differential equations, or the observed convergence order when the exact formula for the global solution is known in prior.

Received by the editors May 29 2019; Accepted June 18 2019; Published online June 25 2019.
2000 *Mathematics Subject Classification.* 65M06,65M12,76D05.
Key words and phrases. Energy-stable method, Second-order method, Incompressible Navier-Stokes equations.
† Corresponding author.

While the convergence order is indirectly measured as mentioned above, the stability of a numerical solution can be clearly stated in L^2 norm. We briefly review the well-known L^2 estimate [1] of the Navier-Stokes equations:

$$\begin{cases} U_t + U \cdot \nabla U &= -\nabla p + \mu \Delta U & \text{in } \Omega \\ \nabla \cdot U &= 0 & \text{in } \Omega \\ U &= 0 & \text{on } \partial\Omega, \end{cases}$$

where Ω denotes a bounded domain with its boundary $\partial\Omega$.

The first equation is the conservation law of momentum, and the last two equations are incompressibility condition and no-slip boundary condition. The above system does not increase the kinetic energy, which is shown below.

$$\begin{aligned} \frac{d}{dt}\left[\int_\Omega \frac{1}{2}U^2\,dx\right] &= \int_\Omega U \cdot \frac{DU}{Dt}\,dx = \int_\Omega U \cdot (-\nabla p + \mu\Delta U)\,dx \\ &= -\int_\Omega \mu \nabla U : \nabla U\,dx \le 0. \end{aligned}$$

Consequently, a numerical solution $U^n \simeq U(x, t^n)$ is said to be ***energy stable***, or L^2 ***stable in the strong sense***, if

$$\left\|U^{n+1}\right\|_{L^2} \le \|U^n\|_{L^2}, \quad \forall n \in \mathbb{N}.$$

We wish to distinguish the L^2 strong stability from the usual definition of L^2 stability. A numerical solution is said to be L^2 stable, if there exists a constant C_T for each time $T > 0$ such that

$$\|U^n\|_{L^2} \le C_T \left\|U^0\right\|_{L^2}, \quad \forall n \in \mathbb{N} \text{ with } \Delta t \cdot n \le T.$$

In practice, the constant C_T, though it may exist, is hard to be measured, so that an increase of L^2 norm, $\left\|U^{n+1}\right\|_{L^2} > \|U^n\|_{L^2}$ may put the users into a puzzle to decide whether it is a sign of numerical instability or it is still within a bound of the weak L^2 stability. From these reasons, the strong stability, or the energy stability, is more desired than the weak stability, and better conforms to the physics.

To the best to our survey, there have been a few studies related to energy stability of the Navier-Stokes equations. G. Amsanay-Alex et al. [3] proposed L^2 stable approximation of the Navier-Stokes equations with variable density. They constructed a finite-volume type discretization based on the kinetic energy in continuous level, but it turned out to be L^2 stable in the inequality sense. Later on, R. Herbin et al. [4] extended this idea adopted to MAC configuration for compressible Navier-Stokes equations, but still not in strong L^2 stable. Recently, M. Gunzburger et al. [5] and A. Takhirov et al. [6] provided L^2 energy stable methods for simulating parameterized flow problems.

The Navier-Stokes equations consist of convection, diffusion and elliptic constraint terms. Being nonlinear, the convection term has been explicitly approximated in most numerical methods. The incompressibility, which is the elliptic constraint, is imposed either at the same time of diffusion process or after that. In the former case, a large-sized linear system, so called

the saddle system [7, 8, 9] needs to be solved, and in the latter case, a series of smaller linear systems, called a projection approach [10, 11, 12, 13], is solved.

When one aims at achieving the strong stability for the system of Navier-Stokes equations, the one would realize that a main difficulty lies on the convection term. As a stand-alone equation apart from the system, the diffusion term is a gradient flow to minimize the L^2 norm, and the elliptic constraint is the Hodge-Helmholtz projection that is orthogonal in L^2 inner product. While the both processes decrease L^2 norm, the convection term conserves it. Consider a linear convection equation with velocity field U that is incompressible and has no-slip boundary condition.

$$\phi_t + U \cdot \nabla \phi = 0 \text{ in } \Omega. \tag{1.1}$$

The conservation of L^2 norm follows from the following estimation:

$$\begin{aligned}
\frac{d}{dt}\left[\int_\Omega \frac{1}{2}\phi^2\, dx\right] &= \int_\Omega \phi \cdot \phi_t\, dx = -\int_\Omega \phi \cdot (U \cdot \nabla \phi)\ dx \\
&= \int_\Omega \nabla \cdot (\phi U)\, \phi\, dx = \int_\Omega \nabla \phi \cdot (U\phi)\ dx \quad (\because \nabla \cdot U = 0) \\
&= 0 \quad \left(\because = -\int_\Omega \nabla \phi \cdot (U\phi)\ dx\right).
\end{aligned}$$

Thus, when we consider a numerical solver for convection equation (1.1), it would be better if a numerical solution $\{\phi^n\}$ to (1.1) is not only L^2 stable in the strong sense, but also L^2 ***preserving*** in the following sense:

$$\|\phi^{n+1}\|_{L^2} = \|\phi^n\|_{L^2}, \quad n \geq 0.$$

In fact, in [1], the authors suggested an explicit method which obtains L^2 stability in the strong sense. However, it was only a first-order accurate method and thus, it was highly dissipative. Therefore, although it actually attains strong L^2 stability, it cannot guarantee the L^2 preserving property. Thus, it is natural to ask about whether it can be accomplished by utilizing second-order method. Unfortunately, standard explicit second-order methods that we tried all failed to be L^2 stable in the strong sense for a pathological counterexample, let alone the L^2 preserving property (See Section 2). Thus, the goal of this paper is two-fold. First, we propose a second-order implicit numerical method for convection equation (1.1) with L^2 preserving property. Then, based on newly introduced solver for convection equation, we suggest a second-order numerical method for the incompressible Navier-Stokes equations, which do attain a strong L^2 stability.

The rest of the paper is organized as follows. In section 2, we report our numerical tests of the standard explicit second-order methods. In section 3 and section 4, we introduce an implicit Runge-Kutta method in time that exactly preserves the kinetic energy for inviscid fluids and does not increase the energy for viscous fluids. In either case, it is L^2 stable in the strong sense.

Since the integration-by-parts in space is essential to achieve the stability, we take the Marker-And-Cell space configuration [14] in rectangular domains to enable the integration-by-parts in discrete level. Section 5 reports numerical tests that validate the stability and accuracy of our proposed method.

2. Investigation on the strong L^2-stability of explicit second order schemes for Convection equation

In this section, we test the strong L^2 stability of famous explicit second-order schemes for convection equation (1.1). As a test subject, we choose three conventional schemes as follows: the Lax-Wendroff scheme, the Jiang-Tadmor (J-T) scheme [15], which is a generalized scheme of the Nessyahu-Tadmor scheme to two-dimensional space, and the second-order essentially non-oscillatory scheme [16] with the Lax-Friedrichs flux (ENO2-LF). To investigate strong L^2 stability of these scheme, we consider the following two-dimensional convection equation on a square domain with the periodic boundary condition

$$\phi_t + \nabla \cdot (U\phi) = 0, \quad (x, y) \in [-1, 1] \times [-1, 1], \quad t \geq 0, \tag{2.1}$$

subjected to the periodic initial data

$$\phi(x, y, 0) = \phi_0(x, y) := \sin(\pi(x + y)). \tag{2.2}$$

We construct an incompressible velocity field $U(x, y) := (u(x, y), v(x, y))$ as a Hodge projection of the velocity field $\tilde{U} := (xy, x^2 - y^2)$ onto the divergence free vector field. Below, we investigate L^2 stability of (2.1)-(2.2) for each explicit schemes. We take a grid size $N = 50$ and CFL number $\lambda = \frac{\Delta t}{\Delta x} = \frac{\Delta t}{\Delta y} = 0.25$ in all the numerical tests below.

• (Case 1) : Lax-Wendroff scheme.

We first study L^2 stability of numerical solution constructed by the Lax-Wendroff scheme. The standard two-dimensional Lax-Wendroff method can be described as the following scheme

$$\begin{aligned}
\phi_{ij}^{n+1} = \phi_{ij}^n &- \frac{\Delta t}{2\Delta x}\left(u_{i+1,j}\phi_{i+1,j} - u_{i-1,j}\phi_{i-1,j}\right) - \frac{\Delta t}{2\Delta y}\left(v_{i,j+1}\phi_{i,j+1} - v_{i,j-1}\phi_{i,j-1}\right) \\
&+ \frac{\Delta t^2}{2\Delta x^2}\left(\frac{u_{i+1,j} + u_{i,j}}{2}(u_{i+1,j}\phi_{i+1,j} - u_{i,j}\phi_{i,j}) - \frac{u_{i,j} + u_{i-1,j}}{2}(u_{i,j}\phi_{i,j} - u_{i-1,j}\phi_{i-1,j})\right) \\
&+ \frac{\Delta t^2}{2\Delta y^2}\left(\frac{u_{i,j+1} + u_{i,j}}{2}(v_{i,j+1}\phi_{i,j+1} - v_{i,j}\phi_{i,j}) - \frac{v_{i,j} + v_{i,j-1}}{2}(v_{i,j}\phi_{i,j} - v_{i,j-1}\phi_{i,j-1})\right) \\
&+ \frac{\Delta t^2}{4\Delta x\Delta y}\left(v_{i,j+1}\left(u_{i+1,j+1}\phi_{i+1,j+1} - u_{i-1,j+1}\phi_{i-1,j+1}\right)\right. \\
&\qquad \left. - v_{i,j-1}\left(u_{i+1,j-1}\phi_{i+1,j-1} - u_{i-1,j-1}\phi_{i-1,j-1}\right)\right).
\end{aligned}$$

Figure 1 shows the dynamics of L^2 norm of the solution to (2.1)-(2.2) with the Lax-Wendroff scheme. As we can observe, L^2 norm of the numerical solution increases with time. Thus, we

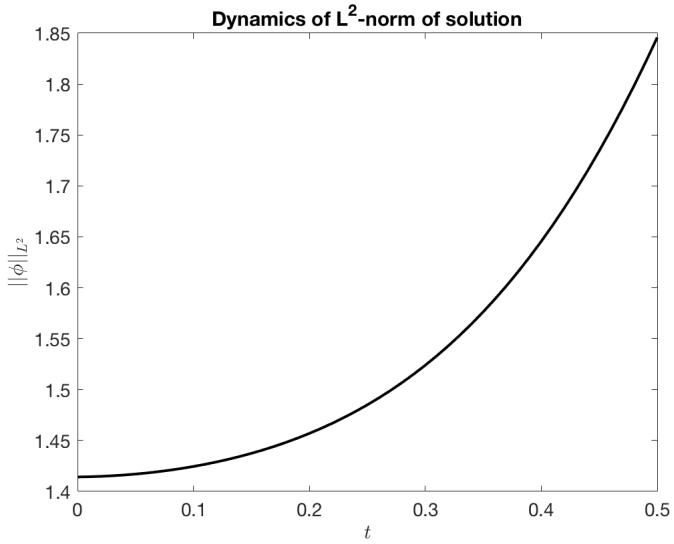

FIGURE 1. Dynamics of L^2 norm for Lax-Wendroff scheme

conclude that the Lax-Wendroff scheme does not attain strong L^2 stability in general.

• (Case 2) : J-T scheme.

Next, we present the result of a numerical test on L^2 stability of J-T scheme. The J-T scheme updates the values at the next time step on the staggered grid points. The exact description for the J-T scheme reads as follows [15]

$$\begin{aligned}
\phi^{n+1}_{i+\frac{1}{2},j+\frac{1}{2}} &= \frac{1}{4}\left(\phi^n_{i,j}+\phi^n_{i+1,j}+\phi^n_{i,j+1}+\phi^n_{i+1,j+1}\right)\\
&\quad+\frac{1}{16}\left(\phi'_{i,j}-\phi'_{i+1,j}\right)-\frac{\Delta t}{2\Delta x}\left[u_{i+1,j}\phi^{n+\frac{1}{2}}_{i+1,j}-u_{i,j}\phi^{n+\frac{1}{2}}_{i,j}\right]\\
&\quad+\frac{1}{16}\left(\phi'_{i,j+1}-\phi'_{i+1,j+1}\right)-\frac{\Delta t}{2\Delta x}\left[u_{i+1,j+1}\phi^{n+\frac{1}{2}}_{i+1,j+1}-u_{i,j+1}\phi^{n+\frac{1}{2}}_{i,j+1}\right]\\
&\quad+\frac{1}{16}\left(\phi'_{i,j}-\phi'_{i,j+1}\right)-\frac{\Delta t}{2\Delta y}\left[v_{i,j+1}\phi^{n+\frac{1}{2}}_{i,j+1}-v_{i,j}\phi^{n+\frac{1}{2}}_{i,j}\right]\\
&\quad+\frac{1}{16}\left(\phi'_{i+1,j}-\phi'_{i+1,j+1}\right)-\frac{\Delta t}{2\Delta y}\left[v_{i+1,j+1}\phi^{n+\frac{1}{2}}_{i+1,j+1}-v_{i+1,j}\phi^{n+\frac{1}{2}}_{i+1,j}\right]
\end{aligned}$$

where the primed values are defined as

$$\phi'_{ij}:=\text{minmod}\left\{\phi^n_{i+1,j}-\phi^n_{i,j},\frac{1}{2}\left(\phi^n_{i+1,j}-\phi^n_{i-1,j}\right),\phi^n_{i,j}-\phi^n_{i-1,j}\right\},$$

$$\phi'_{ij} := \text{minmod}\left\{\phi^n_{i,j+1} - \phi^n_{i,j}, \frac{1}{2}\left(\phi^n_{i,j+1} - \phi^n_{i,j-1}\right), \phi^n_{i,j} - \phi^n_{i,j-1}\right\}$$

and the temporal values at the half step are calculated as

$$\phi^{n+1/2}_{i,j} := \phi^n_{i,j} - \frac{\Delta t}{2\Delta x} u_{i,j}\phi'_{i,j} - \frac{\Delta t}{2\Delta y} v_{i,j}\phi'_{i,j}.$$

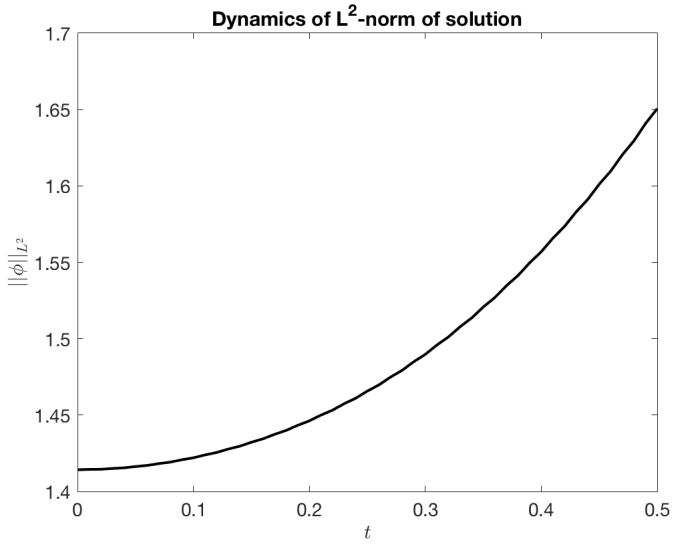

FIGURE 2. Dynamics of L^2 norm for central scheme

Figure 2 illustrates the dynamics of L^2 norm of the J-T scheme. The result is similar to that of the Lax-Wendroff scheme and again we conclude that the J-T scheme also cannot guarantee strong L^2 stability for this example.

• (Case 3) : ENO scheme.

As a final example, we study L^2 stability of ENO scheme. The ENO scheme we tested can be written as the following semi-discrete form

$$\frac{d\phi_{ij}}{dt} = -\frac{1}{\Delta x}\left((u\phi)_{i+\frac{1}{2},j} - (u\phi)_{i-\frac{1}{2},j}\right) - \frac{1}{\Delta y}\left((v\phi)_{i,j+\frac{1}{2}} - (v\phi)_{i,j-\frac{1}{2}}\right)$$

where $u\phi$ is constructed by using ENO2 interpolation $\phi^{\pm}_{i+\frac{1}{2},j}$ at the cell interface with Lax-Friedrichs flux function:

$$(u\phi)_{i+\frac{1}{2},j} := \frac{1}{2}\left(u_{i+\frac{1}{2},j}\left(\phi^+_{i+\frac{1}{2},j} + \phi^-_{i+\frac{1}{2},j}\right) - \alpha\left(\phi^+_{i+\frac{1}{2},j} - \phi^-_{i+\frac{1}{2},j}\right)\right)$$

and $v\phi$ is also defined in a similar manner. Since the maximum velocity in our example is 1, we choose α to be 1. For the time integration, we use the TVD-RK3 time integration [17].

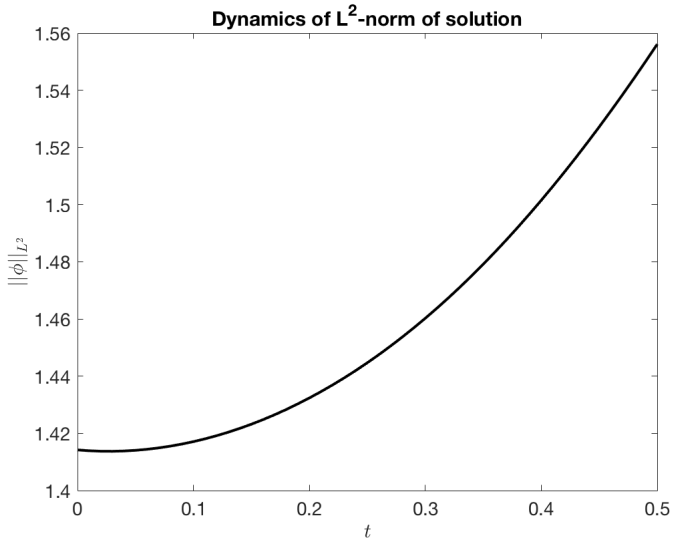

FIGURE 3. Dynamics of L^2 norm for ENO scheme

Figure 3 presents the result of the test on L^2 norm of the solution constructed by the ENO scheme. It resembles the dynamics of L^2 norm of previous two examples and therefore, the ENO scheme also cannot guarantee strong L^2 stability.

According to the several numerical tests above, the well-known second-order schemes sometimes fail to satisfy strong L^2 stability, let alone the possibility of being proved rigorously. However, since strong L^2 stability of the solution is one of the most important physical property of the solution to convection equation (1.1) with incompressible velocity field, a scheme guaranteeing strong L^2 stability is much more appropriate scheme from the physical point of view.

3. MODIFIED IMPLICIT RUNGE-KUTTA METHOD

In the previous section, we reported that many standard explicit second-order methods fail to be L^2 stable in the strong sense for the approximation on the linear advection equation (1.1). In this section, we introduce a second-order implicit method that approximates the linear advection equation $\phi_t + U \cdot \nabla\phi = 0$ with L^2 stability in the strong sense.

With the incompressibility condition on the velocity field U, we may take the conservation form $\phi_t + \nabla \cdot (\phi U) = 0$ of (1.1). Among many candidates, we focus on the following second-order accurate implicit Runge-Kutta method [18].

$$\begin{cases} \phi^{n+\frac{1}{2}} &= \phi^n - \frac{\Delta t}{2} \nabla \cdot \left(\phi^{n+\frac{1}{2}} U \right), \\ \phi^{n+1} &= \phi^n - \Delta t \nabla \cdot \left(\phi^{n+\frac{1}{2}} U \right). \end{cases} \tag{3.1}$$

The main advantage of the semi-discretization form (3.1) is that it satisfies the following L^2 norm preserving property.

Lemma 3.1. *When $\nabla \cdot U = 0$ in Ω and $U \cdot n = 0$ on $\partial\Omega$ are satisfied, the semi-discretization form (3.1) preserves the L^2 norm, i.e.*

$$\left\| \phi^{n+1} \right\|_{L^2} = \left\| \phi^n \right\|_{L^2}.$$

Proof. First, note that $\frac{\phi^{n+\frac{1}{2}} - \phi^n}{\Delta t/2} = \nabla \cdot \left(\phi^{n+\frac{1}{2}} U \right) = \frac{\phi^{n+1} - \phi^n}{\Delta t}$ implies $\phi^{n+\frac{1}{2}} = \frac{\phi^{n+1} + \phi^n}{2}$, and then

$$\begin{aligned} \int_\Omega \frac{\left(\phi^{n+1}\right)^2 - \left(\phi^n\right)^2}{2\Delta t} dx &= \int_\Omega \frac{\phi^{n+1} + \phi^n}{2} \frac{\phi^{n+1} - \phi^n}{\Delta t} dx \\ &= -\int_\Omega \phi^{n+\frac{1}{2}} \nabla \cdot \left(\phi^{n+\frac{1}{2}} U \right) dx \\ &= \int_\Omega \nabla \phi^{n+\frac{1}{2}} \cdot \left(\phi^{n+\frac{1}{2}} U \right) dx \, (\because U \cdot n = 0 \text{ on } \partial\Omega) \\ &= \int_\Omega \left(\nabla \cdot \left(\phi^{n+\frac{1}{2}} U \right) \right) \phi^{n+\frac{1}{2}} \, dx \, (\because \nabla \cdot U = 0 \text{ in } \Omega) \\ &= 0 \quad \left(\because = -\int_\Omega \phi^{n+\frac{1}{2}} \nabla \cdot \left(\phi^{n+\frac{1}{2}} U \right) dx \right). \end{aligned}$$

□

For the above lemma to be valid in the discrete level, the integration-by-parts and the product rule in the discrete level need to be satisfied. For that purpose, we assume a rectangular domain Ω and take the Marker-And-Cell (MAC) space configuration.

As depicted in Figure 4, the velocity field $U = (u, v)$ is sampled on $\left\{ u_{i+\frac{1}{2},j} \right\}$ and $\left\{ v_{i,j+\frac{1}{2}} \right\}$. The incompressibility of the velocity field is defined as

$$\left(\nabla^h \cdot U \right)_{i,j} := \frac{u_{i+\frac{1}{2},j} - u_{i-\frac{1}{2},j}}{\Delta x} + \frac{v_{i,j+\frac{1}{2}} - v_{i,j-\frac{1}{2}}}{\Delta y} = 0. \tag{3.2}$$

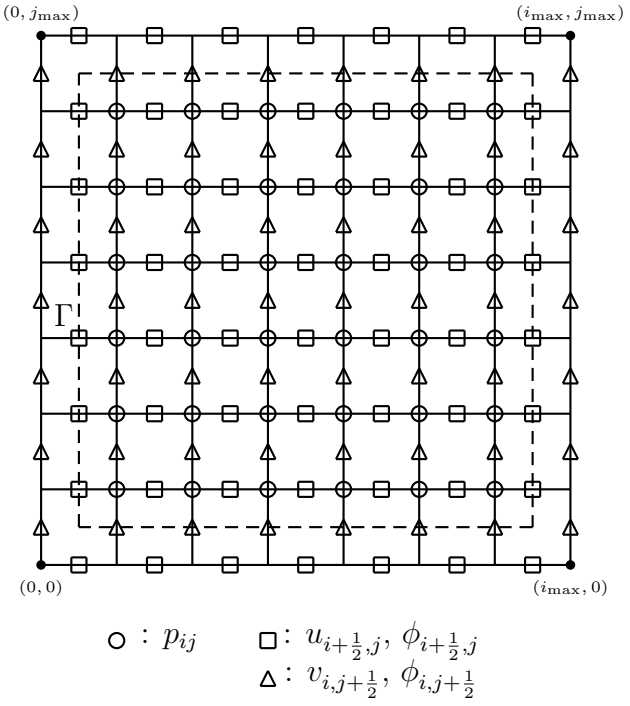

FIGURE 4. MAC configuration

We bear in our mind that the method for solving the linear convection is to be applied to solving the Navier-Stokes equations. Thus, the scalar ϕ is assumed to be sampled either on $\left\{\phi_{i+\frac{1}{2},j}\right\}$ or on $\left\{\phi_{i,j+\frac{1}{2}}\right\}$. Due to the symmetry, it is enough to describe the case $\left\{\phi_{i+\frac{1}{2},j}\right\}$. Utilizing the central finite differences on the MAC configuration, the full discretization of our method is as follows.

$$
\begin{cases}
\phi^{n+\frac{1}{2}}_{i+\frac{1}{2},j} = \phi^{n}_{i+\frac{1}{2},j} - \frac{\Delta t}{2}\nabla\cdot\left(\phi^{n+\frac{1}{2}}U\right)_{i+\frac{1}{2},j} \\
\phi^{n+1}_{i+\frac{1}{2},j} = \phi^{n}_{i+\frac{1}{2},j} - \Delta t\nabla\cdot\left(\phi^{n+\frac{1}{2}}U\right)_{i+\frac{1}{2},j} \\
\nabla\cdot\left(\phi^{n+\frac{1}{2}}U\right)_{i+\frac{1}{2},j} := \left(\frac{u_{i+\frac{3}{2},j}+u_{i+\frac{1}{2},j}}{2}\frac{\phi^{n+\frac{1}{2}}_{i+\frac{3}{2},j}+\phi^{n+\frac{1}{2}}_{i+\frac{1}{2},j}}{2} - \frac{u_{i+\frac{1}{2},j}+u_{i-\frac{1}{2},j}}{2}\frac{\phi^{n+\frac{1}{2}}_{i+\frac{1}{2},j}+\phi^{n+\frac{1}{2}}_{i-\frac{1}{2},j}}{2}\right)\frac{1}{\Delta x} \\
+\left(\frac{v_{i+1,j+\frac{1}{2}}+v_{i,j+\frac{1}{2}}}{2}\frac{\phi^{n+\frac{1}{2}}_{i+\frac{1}{2},j+1}+\phi^{n+\frac{1}{2}}_{i+\frac{1}{2},j}}{2} - \frac{v_{i+1,j-\frac{1}{2}}+v_{i,j-\frac{1}{2}}}{2}\frac{\phi^{n+\frac{1}{2}}_{i+\frac{1}{2},j}+\phi^{n+\frac{1}{2}}_{i+\frac{1}{2},j-1}}{2}\right)\frac{1}{\Delta y}
\end{cases}
\tag{3.3}
$$

With the discrete incompressibility condition (3.2), the above full discretization can be simplified as follows.

$$\begin{aligned}\phi^{n}_{i+\frac{1}{2},j} = \phi^{n+\frac{1}{2}}_{i+\frac{1}{2},j} &+ \frac{\triangle t}{8\triangle x}\left(u_{i+\frac{3}{2},j}+u_{i+\frac{1}{2},j}\right)\phi^{n+\frac{1}{2}}_{i+\frac{3}{2},j} - \frac{\triangle t}{8\triangle x}\left(u_{i+\frac{1}{2},j}+u_{i-\frac{1}{2},j}\right)\phi^{n+\frac{1}{2}}_{i-\frac{1}{2}j}\\ &+ \frac{\triangle t}{8\triangle y}\left(v_{i+1,j+\frac{1}{2}}+v_{i,j+\frac{1}{2}}\right)\phi^{n+\frac{1}{2}}_{i+\frac{1}{2},j+1} - \frac{\triangle t}{8\triangle y}\left(v_{i+1,j-\frac{1}{2}}+v_{i,j-\frac{1}{2}}\right)\phi^{n+\frac{1}{2}}_{i+\frac{1}{2},j-1}\\ \phi^{n+1}_{i+\frac{1}{2}j} &= 2\phi^{n+\frac{1}{2}}_{i+\frac{1}{2}j} - \phi^{n}_{i+\frac{1}{2}j}.\end{aligned}$$

If we regard ϕ^n and $\phi^{n+\frac{1}{2}}$ as a vector in $\mathbb{R}^{(i_{max}-1)j_{max}}$, then the first step can be written as the following linear equation:

$$A\phi^{n+\frac{1}{2}} = \phi^{n},$$

where $\left\{\phi^{n}_{i+\frac{1}{2},j}\right\}, \left\{\phi^{n+\frac{1}{2}}_{i+\frac{1}{2},j}\right\} \in \mathbb{R}^{(i_{max}-1)j_{max}}$ and the matrix A is defined by

$$A_{(i+\frac{1}{2},j),(\tilde{i}+\frac{1}{2},\tilde{j})} := \begin{cases} 1 & \text{if} \quad \tilde{i}=i \quad \text{and} \quad \tilde{j}=j,\\ -\frac{\triangle t}{8\triangle x}\left(u_{i+\frac{1}{2},j}+u_{i-\frac{1}{2},j}\right) & \text{if} \quad \tilde{i}=i-1 \quad \text{and} \quad \tilde{j}=j,\\ \frac{\triangle t}{8\triangle x}\left(u_{i+\frac{3}{2},j}+u_{i+\frac{1}{2},j}\right) & \text{if} \quad \tilde{i}=i+1 \quad \text{and} \quad \tilde{j}=j,\\ -\frac{\triangle t}{8\triangle y}\left(v_{i+1,j-\frac{1}{2}}+v_{i,j-\frac{1}{2}}\right) & \text{if} \quad \tilde{i}=i \quad \text{and} \quad \tilde{j}=j-1,\\ \frac{\triangle t}{8\triangle y}\left(v_{i+1,j+\frac{1}{2}}+v_{i,j+\frac{1}{2}}\right) & \text{if} \quad \tilde{i}=i \quad \text{and} \quad \tilde{j}=j+1,\\ 0 & \text{if} \quad otherwise. \end{cases} \tag{3.4}$$

Before we address the L^2 preserving of the scheme, we first prove the matrix A is non-singular so that $\phi^{n+\frac{1}{2}}$ is well-defined under the appropriate CFL condition.

Lemma 3.2 (Solvability)**.** *The matrix A given in (3.4) is invertible under the CFL condition $\triangle t < \frac{\min\{\triangle x,\triangle y\}}{\max\{\|u\|_\infty,\|v\|_\infty\}}$.*

Proof. The proof follows from the direct application of Gershgorin circle theorem. Note that the following holds for every $1 \le i \le N$:

$$\begin{aligned}\sum_{j\neq i}|a_{i,j}| &= \frac{\triangle t}{8\triangle x}\left(\left|u_{i+\frac{1}{2}j}+u_{i-\frac{1}{2}j}\right| + \left|u_{i+\frac{3}{2}j}+u_{i+\frac{1}{2}j}\right|\right)\\ &\quad + \frac{\triangle t}{8\triangle y}\left(\left|v_{i+1j-\frac{1}{2}}+v_{ij-\frac{1}{2}}\right| + \left|v_{i+1j+\frac{1}{2}}+v_{ij+\frac{1}{2}}\right|\right)\\ &\le \frac{\triangle t}{2\triangle x}\|u\|_\infty + \frac{\triangle t}{2\triangle y}\|v\|_\infty\\ &< 1 = |a_{i,i}|.\end{aligned}$$

Hence, the Gershgorin circle theorem guarantees the invertibility of A. □

Next, we provide the L^2 preserving property of the modified implicit RK2 method (3.3).

Theorem 3.1 (L^2 preserving)**.** *For every* $n \in \mathbb{N}$, $\|\phi^{n+1}\|_{L^2} = \|\phi^n\|_{L^2}$.

Proof. Let $\langle\ ,\ \rangle$ be the standard inner-product in $\mathbb{R}^{(i_{max}-1)j_{max}}$. Regarding $\nabla\cdot(\phi^{n+\frac{1}{2}}U)$ as a vector in $\mathbb{R}^{(i_{max}-1)j_{max}}$, we can obtain

$$\begin{aligned}
&\langle\phi^{n+1},\phi^{n+1}\rangle\\
&= \langle\phi^n,\phi^n\rangle + 2\triangle t\left\langle\phi^n,\nabla\cdot(\phi^{n+\frac{1}{2}}U)\right\rangle + \triangle t^2\left\langle\nabla\cdot(\phi^{n+\frac{1}{2}}U),\nabla\cdot(\phi^{n+\frac{1}{2}}U)\right\rangle\\
&= \langle\phi^n,\phi^n\rangle + 2\triangle t\left\langle\phi^{n+\frac{1}{2}} - \frac{\triangle t}{2}\nabla\cdot(\phi^{n+\frac{1}{2}}U),\nabla\cdot(\phi^{n+\frac{1}{2}}U)\right\rangle\\
&\qquad + \triangle t^2\left\langle\nabla\cdot(\phi^{n+\frac{1}{2}}U),\nabla\cdot(\phi^{n+\frac{1}{2}}U)\right\rangle\\
&= \langle\phi^n,\phi^n\rangle + 2\triangle t\left\langle\phi^{n+\frac{1}{2}},\nabla\cdot(\phi^{n+\frac{1}{2}}U)\right\rangle.
\end{aligned}$$

Thus, it suffices to show that $\langle\phi^{n+\frac{1}{2}},\nabla\cdot(\phi^{n+\frac{1}{2}}U)\rangle = 0$. However, it can be estimated as

$$\begin{aligned}
\left\langle\phi^{n+\frac{1}{2}},\nabla\cdot\left(\phi^{n+\frac{1}{2}}U\right)\right\rangle &= \sum_{i=1}^{i_{max}-2}\sum_{j=1}^{j_{max}-1}\phi^{n+\frac{1}{2}}_{i+\frac{1}{2},j}(\nabla\cdot(\phi^{n+\frac{1}{2}}U))_{i+\frac{1}{2},j}\\
&= \sum_{i=1}^{i_{max}-2}\sum_{j=1}^{j_{max}-1}\frac{\phi^{n+\frac{1}{2}}_{i+\frac{1}{2},j}}{\triangle x}\left(\frac{\phi^{n+\frac{1}{2}}_{i+\frac{3}{2},j}+\phi^{n+\frac{1}{2}}_{i+\frac{1}{2},j}}{2}\frac{u_{i+\frac{3}{2},j}+u_{i+\frac{1}{2},j}}{2}\right.\\
&\qquad\left.-\frac{\phi^{n+\frac{1}{2}}_{i+\frac{1}{2},j}+\phi^{n+\frac{1}{2}}_{i-\frac{1}{2},j}}{2}\frac{u_{i+\frac{1}{2},j}+u_{i-\frac{1}{2},j}}{2}\right)\\
&\quad+\sum_{i=1}^{i_{max}-2}\sum_{j=1}^{j_{max}-1}\frac{\phi^{n+\frac{1}{2}}_{i+\frac{1}{2},j}}{\triangle y}\left(\frac{\phi^{n+\frac{1}{2}}_{i+\frac{1}{2},j+1}+\phi^{n+\frac{1}{2}}_{i+\frac{1}{2},j}}{2}\frac{v_{i+1,j+\frac{1}{2}}+v_{i,j+\frac{1}{2}}}{2}\right.\\
&\qquad\left.-\frac{\phi^{n+\frac{1}{2}}_{i+\frac{1}{2},j}+\phi^{n+\frac{1}{2}}_{i+\frac{1}{2},j-1}}{2}\frac{v_{i+1,j-\frac{1}{2}}+v_{i,j-\frac{1}{2}}}{2}\right)\\
&=: \mathcal{I}_1+\mathcal{I}_2.
\end{aligned}$$

We estimate $\mathcal{I}_1$ and $\mathcal{I}_2$ separately as follows:

• (Estimates for $\mathcal{I}_1$) : For $\mathcal{I}_1$, we have

$$\begin{aligned}\mathcal{I}_1 &= \sum_{i=1}^{i_{max}-3}\sum_{j=1}^{j_{max}-1}\frac{\phi^{n+\frac{1}{2}}_{i+\frac{1}{2},j}\phi^{n+\frac{1}{2}}_{i+\frac{3}{2},j}}{2\triangle x}\frac{u_{i+\frac{3}{2},j}+u_{i+\frac{1}{2},j}}{2} - \sum_{i=2}^{i_{max}-2}\sum_{j=1}^{j_{max}-1}\frac{\phi^{n+\frac{1}{2}}_{i+\frac{1}{2},j}\phi^{n+\frac{1}{2}}_{i-\frac{1}{2},j}}{2\triangle x}\frac{u_{i+\frac{1}{2},j}+u_{i-\frac{1}{2},j}}{2}\\ &+ \sum_{i=1}^{i_{max}-2}\sum_{j=1}^{j_{max}-1}\frac{\left(\phi^{n+\frac{1}{2}}_{i+\frac{1}{2},j}\right)^2}{4}\left(\frac{u_{i+\frac{3}{2},j}-u_{i+\frac{1}{2},j}}{\triangle x}+\frac{u_{i+\frac{1}{2},j}-u_{i-\frac{1}{2},j}}{\triangle x}\right)\\ &= \sum_{i=1}^{i_{max}-2}\sum_{j=1}^{j_{max}-1}\frac{\left(\phi^{n+\frac{1}{2}}_{i+\frac{1}{2},j}\right)^2}{4}\left(\frac{u_{i+\frac{3}{2},j}-u_{i+\frac{1}{2},j}}{\triangle x}+\frac{u_{i+\frac{1}{2},j}-u_{i-\frac{1}{2},j}}{\triangle x}\right).\end{aligned}$$

• (Estimates for $\mathcal{I}_2$) : For $\mathcal{I}_2$,

$$\begin{aligned}\mathcal{I}_2 &= \sum_{i=1}^{i_{max}-2}\sum_{j=1}^{j_{max}-2}\frac{\phi^{n+\frac{1}{2}}_{i+\frac{1}{2},j}}{\triangle y}\left(\frac{\phi^{n+\frac{1}{2}}_{i+\frac{1}{2},j+1}+\phi^{n+\frac{1}{2}}_{i+\frac{1}{2},j}}{2}\frac{v_{i+1,j+\frac{1}{2}}+v_{i,j+\frac{1}{2}}}{2}\right)\\ &- \sum_{i=1}^{i_{max}-2}\sum_{j=2}^{j_{max}-1}\frac{\phi^{n+\frac{1}{2}}_{i+\frac{1}{2},j}}{\triangle y}\left(\frac{\phi^{n+\frac{1}{2}}_{i+\frac{1}{2},j}+\phi^{n+\frac{1}{2}}_{i+\frac{1}{2},j-1}}{2}\frac{v_{i+1,j-\frac{1}{2}}+v_{i,j-\frac{1}{2}}}{2}\right)\\ &= \sum_{i=1}^{i_{max}-2}\sum_{j=2}^{j_{max}-2}\frac{\left(\phi^{n+\frac{1}{2}}_{i+\frac{1}{2},j}\right)^2}{4}\left(\frac{v_{i+1,j+\frac{1}{2}}-v_{i+1,j-\frac{1}{2}}}{\triangle y}+\frac{v_{i,j+\frac{1}{2}}-v_{i,j-\frac{1}{2}}}{\triangle y}\right)\\ &+ \sum_{i=1}^{i_{max}-2}\frac{\left(\phi^{n+\frac{1}{2}}_{i+\frac{1}{2},1}\right)^2}{4}\frac{v_{i+1,\frac{3}{2}}+v_{i,\frac{3}{2}}}{\triangle y} - \frac{\left(\phi^{n+\frac{1}{2}}_{i+\frac{1}{2},M-1}\right)^2}{4}\frac{v_{i+1,M-\frac{3}{2}}+v_{i,M-\frac{3}{2}}}{\triangle y}.\end{aligned}$$

It follows from the discrete boundary condition that

$$\begin{aligned}
&\sum_{i=1}^{i_{max}-2} \frac{\left(\phi^{n+\frac{1}{2}}_{i+\frac{1}{2},1}\right)^2}{4} \frac{v_{i+1,\frac{3}{2}} + v_{i,\frac{3}{2}}}{\triangle y} - \frac{\left(\phi^{n+\frac{1}{2}}_{i+\frac{1}{2},M-1}\right)^2}{4} \frac{v_{i+1,M-\frac{3}{2}} + v_{i,M-\frac{3}{2}}}{\triangle y} \\
&= \sum_{i=1}^{i_{max}-2} \frac{\left(\phi^{n+\frac{1}{2}}_{i+\frac{1}{2},1}\right)^2}{4} \left(\frac{v_{i+1,\frac{3}{2}} - v_{i+1,\frac{1}{2}}}{\triangle y} + \frac{v_{i,\frac{3}{2}} - v_{i,\frac{1}{2}}}{\triangle y} \right) \\
&+ \sum_{i=1}^{i_{max}-2} \frac{\left(\phi^{n+\frac{1}{2}}_{i+\frac{1}{2},M-1}\right)^2}{4} \left(\frac{v_{i+1,M-\frac{1}{2}} - v_{i+1,M-\frac{3}{2}}}{\triangle y} + \frac{v_{i,M-\frac{1}{2}} - v_{i,M-\frac{3}{2}}}{\triangle y} \right),
\end{aligned}$$

which yields

$$\mathcal{I}_2 = \sum_{i=1}^{i_{max}-2} \sum_{j=1}^{j_{max}-1} \frac{\left(\phi^{n+\frac{1}{2}}_{i+\frac{1}{2},j}\right)^2}{4} \left(\frac{v_{i+1,j+\frac{1}{2}} - v_{i+1,j-\frac{1}{2}}}{\triangle y} + \frac{v_{i,j+\frac{1}{2}} - v_{i,j-\frac{1}{2}}}{\triangle y} \right).$$

Therefore, we use the discrete divergence condition to conclude that

$$\mathcal{I}_1 + \mathcal{I}_2 = 0.$$

This implies our desired result. □

Remark. (Comment on Explicit RK2)
If we adopt an explicit scheme, i.e.

$$\begin{cases} \phi^{n+\frac{1}{2}} &= \phi^n - \frac{\triangle t}{2} \nabla \cdot (\phi^n U), \\ \phi^{n+1} &= \phi^n - \triangle t \nabla \cdot (\phi^{n+\frac{1}{2}} U), \end{cases}$$

then, the L^2 norm at the $(n+1)$-th step can be estimated as

$$\begin{aligned}
\langle \phi^{n+1}, \phi^{n+1} \rangle &= \langle \phi^n, \phi^n \rangle + \frac{(\triangle t)^4}{4} \langle \nabla \cdot (U \nabla \cdot (\phi^n U)), \nabla \cdot (U \nabla \cdot (\phi^n U)) \rangle \\
&\geq \langle \phi^n, \phi^n \rangle.
\end{aligned}$$

Thus, we can not expect the strong L^2 stability of the scheme.

4. MODIFIED IMPLICIT RK2 METHOD FOR THE INCOMPRESSIBLE NAVIER-STOKES EQUATIONS

Based on the previous section, we present the implicit RK2 discretization for the incompressible Navier-Stokes equations:

$$\begin{cases} U_t + (U \cdot \nabla) U = -\nabla p + \mu \triangle U & \text{in } \Omega, \\ \nabla \cdot U = 0 & \text{in } \Omega, \\ U = 0 & \text{on } \partial\Omega. \end{cases}$$

In order to take advantage of implicit RK2 method, we constructed the following saddle system type 2-step time discretization.

$$\begin{array}{ll} \text{1st step :} & \begin{cases} \frac{U^{n+\frac{1}{2}} - U^n}{\triangle t/2} + \left(V^{n+\frac{1}{2}} \cdot \nabla\right) U^{n+\frac{1}{2}} = -\nabla p^{n+\frac{1}{2}} + \mu \triangle U^{n+\frac{1}{2}} & \text{in } \Omega, \\ \nabla \cdot U^{n+\frac{1}{2}} = 0 \end{cases} \\ \text{2nd step :} & U^{n+1} = 2U^{n+\frac{1}{2}} - U^n \qquad \text{in } \Omega. \end{array} \tag{4.1}$$

Here, $V^{n+\frac{1}{2}}$ is extrapolated as below to mitigate the nonliearity:

$$V^{n+\frac{1}{2}} = U^n + \frac{\triangle t}{2} \frac{U^n - U^{n-1}}{t^n - t^{n-1}}.$$

The following theorem guarantees the L^2 energy stability of above time discretization.

Theorem 4.1 (L^2 energy stability of time discretization)**.** *Let U^{n+1} be generated from U^n by the time discretization (4.1). Then $\left\|U^{n+1}\right\| \leq \|U^n\|$.*

Proof. With $\nabla \cdot U^{n+\frac{1}{2}} = 0$ and integration-by-parts, we have

$$\begin{aligned} \left\|U^{n+1}\right\|^2 - \|U^n\|^2 &= \left\langle U^{n+1} + U^n, U^{n+1} - U^n \right\rangle \\ &= -\triangle t \left\langle 2U^{n+\frac{1}{2}}, \left(V^{n+\frac{1}{2}} \cdot \nabla\right) U^{n+\frac{1}{2}} + \nabla p^{n+\frac{1}{2}} - \mu \triangle U^{n+\frac{1}{2}} \right\rangle \\ &= -2\triangle t \left[\left\langle U^{n+\frac{1}{2}}, \left(V^{n+\frac{1}{2}} \cdot \nabla\right) U^{n+\frac{1}{2}} \right\rangle + \left\langle U^{n+\frac{1}{2}}, \nabla p^{n+\frac{1}{2}} \right\rangle \right. \\ &\qquad \left. - \mu \left\langle U^{n+\frac{1}{2}}, \triangle U^{n+\frac{1}{2}} \right\rangle \right] \\ &= -2\triangle t \left[0 - \left\langle \nabla \cdot U^{n+\frac{1}{2}}, p^{n+\frac{1}{2}} \right\rangle + \mu \left\langle \nabla U^{n+\frac{1}{2}}, \nabla U^{n+\frac{1}{2}} \right\rangle \right] \\ &= -2\triangle t \mu \left\| \nabla U^{n+\frac{1}{2}} \right\|^2 \leq 0. \end{aligned}$$

Here, we utilized the fact that $U^{n+1} = 2U^{n+\frac{1}{2}} - U^n$ equals to

$$\frac{U^{n+1} - U^n}{\triangle t} + \left(V^{n+\frac{1}{2}} \cdot \nabla\right) U^{n+\frac{1}{2}} = -\nabla p^{n+\frac{1}{2}} + \mu \triangle U^{n+\frac{1}{2}}.$$

□

The first system in (4.1) can be written as the following large linear saddle system:

$$\begin{bmatrix} I + \frac{\triangle t}{2}\left(V^{n+\frac{1}{2}} \cdot \nabla\right) - \frac{\triangle t}{2}\mu\triangle & \frac{\triangle t}{2}\nabla \\ \nabla\cdot & O \end{bmatrix} \begin{bmatrix} U^{n+\frac{1}{2}} \\ p^{n+\frac{1}{2}} \end{bmatrix} = \begin{bmatrix} U^n \\ \mathbf{0} \end{bmatrix}. \tag{4.2}$$

In order to solve this system, we need to specify the space discretization of (4.1). Since the discrete version of integration-by-parts is essential for discrete L^2 energy stability, we selected the centered finite difference approximation based on MAC configuration for the space discretization. For example, let $u^{n+\frac{1}{2}}$ be the x-component of $U^{n+\frac{1}{2}}$ with $V^{n+\frac{1}{2}} = \left(u^{n+\frac{1}{2},f}, v^{n+\frac{1}{2},f}\right)$. Here, the superscription f indicates that the variable is a frozen coefficient. Then, system (4.2) reads as

$$\begin{aligned} & u^{n+\frac{1}{2}}_{i+\frac{1}{2},j} + \frac{\triangle t}{2}\left[\frac{1}{\triangle x}\left(\frac{u^{n+\frac{1}{2},f}_{i+\frac{3}{2},j} + u^{n+\frac{1}{2},f}_{i+\frac{1}{2},j}}{2} \cdot \frac{u^{n+\frac{1}{2}}_{i+\frac{3}{2},j} + u^{n+\frac{1}{2}}_{i+\frac{1}{2},j}}{2} - \frac{u^{n+\frac{1}{2},f}_{i+\frac{1}{2},j} + u^{n+\frac{1}{2},f}_{i-\frac{1}{2},j}}{2} \cdot \frac{u^{n+\frac{1}{2}}_{i+\frac{1}{2},j} + u^{n+\frac{1}{2}}_{i-\frac{1}{2},j}}{2}\right)\right. \\ & \left. + \frac{1}{\triangle y}\left(\frac{v^{n+\frac{1}{2},f}_{i+1,j+\frac{1}{2}} + v^{n+\frac{1}{2},f}_{i,j+\frac{1}{2}}}{2} \cdot \frac{u^{n+\frac{1}{2}}_{i+\frac{1}{2},j+1} + u^{n+\frac{1}{2}}_{i+\frac{1}{2},j}}{2} - \frac{v^{n+\frac{1}{2},f}_{i+1,j-\frac{1}{2}} + v^{n+\frac{1}{2},f}_{i,j-\frac{1}{2}}}{2} \cdot \frac{u^{n+\frac{1}{2}}_{i+\frac{1}{2},j} + u^{n+\frac{1}{2}}_{i+\frac{1}{2},j-1}}{2}\right)\right] \\ & - \frac{\triangle t}{2}\mu\left[\frac{1}{(\triangle x)^2}\left(u^{n+\frac{1}{2}}_{i+\frac{3}{2},j} - 2u^{n+\frac{1}{2}}_{i+\frac{1}{2},j} + u^{n+\frac{1}{2}}_{i-\frac{1}{2},j}\right) + \frac{1}{(\triangle y)^2}\left(u^{n+\frac{1}{2}}_{i+\frac{1}{2},j+1} - 2u^{n+\frac{1}{2}}_{i+\frac{1}{2},j} + u^{n+\frac{1}{2}}_{i+\frac{1}{2},j-1}\right)\right] \\ & + \frac{\triangle t}{2}\frac{1}{\triangle x}\left(p^{n+\frac{1}{2}}_{i+1,j} - p^{n+\frac{1}{2}}_{ij}\right) = u^n_{i+\frac{1}{2},j}. \end{aligned}$$

A frozen coefficient $V^{n+\frac{1}{2}}$ is set to be a second-order accurate extrapolation of U^n and U^{n-1}. To minimize the error induced by the initial guess $V^{\frac{1}{2}}$, we solve the 1st step of (4.2) about five times prior to the main iteration and set this solution to be $V^{\frac{1}{2}}$. This technique was suggested in Brown et.al [13]. The nonsymmetric saddle system (4.2) is solved by the General Minimal RESidual (GMRES). We finalize this section with the following theorem on L^2 energy stability in full discretization.

Theorem 4.2 (L^2 energy stability of full discretization)**.** *Let U^{n+1} be generated from U^n by the full discretization of (4.1). Then $\left\|U^{n+1}\right\| \leq \|U^n\|$.*

Proof. From Theorem 3.1 and Theorem 4.1, it suffices to show that discrete version of integration-by-parts for $\left\langle U^{n+\frac{1}{2}}, \nabla p^{n+\frac{1}{2}}\right\rangle$, $\left\langle U^{n+\frac{1}{2}}, \triangle U^{n+\frac{1}{2}}\right\rangle$ hold. Note that these two inner products are

type of $\langle U, -\nabla f\rangle$ for a vector field $U = (u, v)$ and a scalar field f. With the boundary condition $U = 0$ and index shifting in MAC configuration, we obtain

$$\begin{aligned}
\left\langle u, -\frac{\partial f}{\partial x}\right\rangle &:= \sum_{i=1}^{i_{\max}-2}\sum_{j=1}^{j_{\max}-1} u_{i+\frac{1}{2},j}\frac{-f_{i+1,j}+f_{i,j}}{\triangle x} \\
&= -\sum_{i=2}^{i_{\max}-1}\sum_{j=1}^{j_{\max}-1} u_{i-\frac{1}{2},j}\frac{f_{i,j}}{\triangle x} + \sum_{i=1}^{i_{\max}-2}\sum_{j=1}^{j_{\max}-1} u_{i+\frac{1}{2},j}\frac{f_{i,j}}{\triangle x} \\
&= -\sum_{i=1}^{i_{\max}-1}\sum_{j=1}^{j_{\max}-1} u_{i-\frac{1}{2},j}\frac{f_{i,j}}{\triangle x} + \sum_{i=1}^{i_{\max}-1}\sum_{j=1}^{j_{\max}-1} u_{i+\frac{1}{2},j}\frac{f_{i,j}}{\triangle x} \\
&\left(\because u_{i+\frac{1}{2},j} = u_{i_{\max}-\frac{3}{2},j} = 0\right) \\
&= \sum_{i=1}^{i_{\max}-1}\sum_{j=1}^{j_{\max}-1} \frac{u_{i+\frac{1}{2},j} - u_{i-\frac{1}{2},j}}{\triangle x} f_{i,j} \\
&\doteq \left\langle \frac{\partial u}{\partial x}, f\right\rangle.
\end{aligned}$$

In a simliar way, we can show that $\left\langle v, -\frac{\partial f}{\partial y}\right\rangle = \left\langle \frac{\partial v}{\partial y}, f\right\rangle$ in a discrete sense. □

Remark. (Solvability of the saddle system)

Let $A^h x^h = b^h$ be the full discretized saddle system (4.2) and $\hat{x} = \begin{bmatrix}\hat{U}\\ \hat{p}\end{bmatrix}$ be a solution of this system. Then one can easily check that $\tilde{x} = \begin{bmatrix}\hat{U}\\ \hat{p}+c\end{bmatrix}$ is also in a solution space of A^h for any constant c. To handle this singularity, we projected b^h onto a range space of A^h. After this projection, the solvability of (4.2) heavily depends on the nonlinear convection part $I + \frac{\triangle t}{2}\left(V^{n+\frac{1}{2}}\cdot\nabla\right)$. Hence, $\triangle t \le \frac{\min\{\triangle x, \triangle y\}}{\max\left\{\|u\|_\infty, \|v\|_\infty\right\}}$ as in Lemma 3.2 is a proper choice of the proposed method.

5. NUMERICAL EXPERIMENTS

In this section, we perform several numerical experiments to verify the stability and accuracy in two and three dimensions of our method. Throughout this section, the saddle system (4.2) is solved by the restarted GMRES(10). All of the following computations were run on a regular personal computer (8GB RAM and 2.1GHz CPU).

5.1. **Single Vortex in 2D.** We begin with an example that confirms the second-order accuracy of the proposed method. Let us consider a single vortex problem in a domain $\Omega = \left[-\frac{\pi}{2}, \frac{\pi}{2}\right] \times$

$\left[-\frac{\pi}{2}, \frac{\pi}{2}\right]$, with a homogeneous Dirichlet boundary condition. An exact solution to this problem is given by

$$\begin{aligned} u(x, y, t) &= -\cos(x)\sin(y)\cos(t), \\ v(x, y, t) &= \sin(x)\cos(y)\cos(t), \\ p(x, y, t) &= -\frac{1}{4}\cos^2(t)\left(\cos(2x) + \cos(2y)\right), \end{aligned}$$

with a corresponding source term $F = (f_1, f_2)$ where

$$\begin{aligned} f_1 &= -\cos(x)\sin(y)\left(2\cos(t) - \sin(t)\right), \\ f_2 &= \sin(x)\cos(t)\left(2\cos(t) - \sin(t)\right). \end{aligned}$$

Since the energy stability of our method is not relevant to the external force, we utilize the sourcing term only for the accuracy test. Table 1 shows the second-order accuracy of the velocity field in the L^∞ norm.

Grid resolution	$\|u(x,y) - u_{i+\frac{1}{2}j}\|_{L^\infty}$	Order
16×16	3.41×10^{-2}	
32×32	7.89×10^{-3}	2.11
64×64	1.90×10^{-3}	2.05
128×128	4.66×10^{-4}	2.02
256×256	1.14×10^{-4}	2.03

TABLE 1. Accuracy of the velocity U in the L^∞ norm of a single vortex in $\mathbb{R}^2$

5.2. **Single Vortex in 3D.** The exact solution of a three dimensional single vortex problem is given by

$$\begin{aligned} u(x, y, z, t) &= -2\cos(t)\cos(x)\sin(y)\sin(z), \\ v(x, y, z, t) &= \cos(t)\sin(x)\cos(y)\sin(z), \\ w(x, y, z, t) &= \cos(t)\sin(x)\sin(y)\cos(z), \\ p(x, y, z, t) &= \frac{1}{4}\cos^2(t)\left(2\cos(2x) + \cos(2y) + \cos(2z)\right) \end{aligned}$$

in a domain $\Omega = \left[-\frac{\pi}{2}, \frac{\pi}{2}\right]^3$. Table 2 demonstrates that our method retains the second-order accuracy of the velocity field in the L^∞ norm.

Grid resolution	$\|u(x,y,z) - u_{i+\frac{1}{2}jk}\|_{L^\infty}$	Order
$16 \times 16 \times 16$	3.42×10^{-2}	
$32 \times 32 \times 32$	8.13×10^{-3}	2.07
$64 \times 64 \times 64$	1.96×10^{-3}	2.05

TABLE 2. Accuracy of the velocity U in the L^∞ norm of a single vortex in $\mathbb{R}^3$

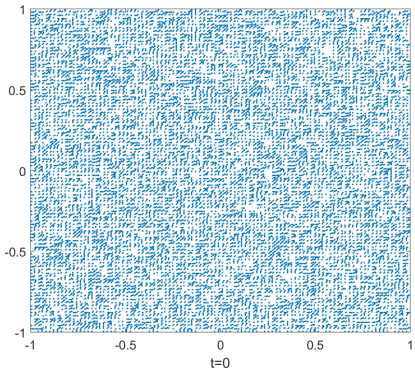

(a) Plot of the initial velocity field

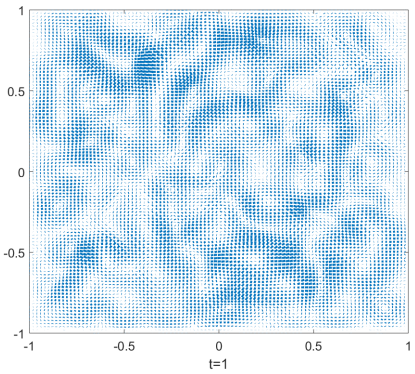

(b) Plot of the velocity field at $t = 1$ by modified Lax-Friedrich

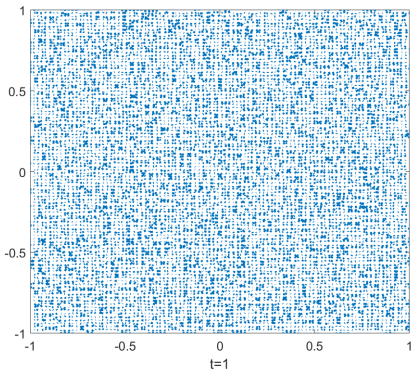

(c) Plot of the velocity field at $t = 1$ by modified implict RK2

FIGURE 5. Plots of (a) initial velocity field of salt-and-pepper noise and the velocity field at $t = 1$ computed by (b) modified Lax-Friedrichs in [1] and (c) modified Implicit RK2.

5.3. **Salt-and-Pepper noise.** This example was first introduced in [1]. The initial velocity U^0 is randomly selected as either 0 or 1 (component-wise) in the domain $\Omega = [-1, 1] \times [-1, 1]$ and then projected onto the divergence-free vector field. A flow generated by this velocity is assumed to be nonviscous with the unit density: $\mu = 0$, $\rho = 1$.

The lack of viscosity to smooth out discontinuities in the velocity field makes it hard to solve this problem numerically. Also, from Theorem 4.2, the L^2 energy of nonviscous flow must be conserved. We tested this problem with the modified implicit RK2 to validate the energy preserving nature of the proposed method. We present the velocity profile at $t = 1$

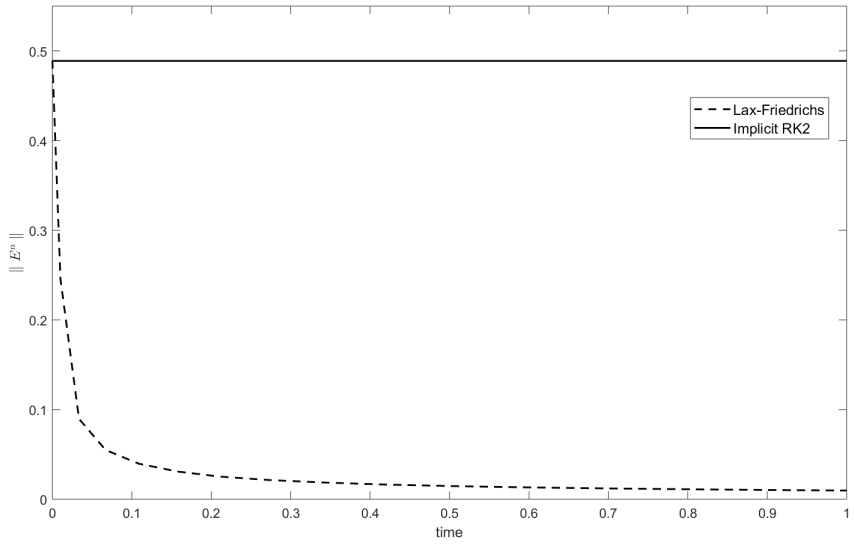

FIGURE 6. Graphs for the energy of a salt-and-pepper noise problem on 100×100 grid by modified Lax-Friedrichs and modified implicit RK2. This indicates that the energy computed by modified implicit RK2 is conserved while that of modified LF is diminished.

on 100×100 grid and the corresponding L^2 energy in Figure 5 and 6, respectively. For a comparison purpose, the results from Lee et. al [1] is also presented in the same figures.

While numerical results from [1] show the nonphysical L^2 energy decay, proposed implicit RK2 method exactly preserve physical L^2 energy conservation. The reason behind the non-physical aspect of the method proposed in [1] is that Lax-Friedrichs type methods introduce an artificial dissipation. This can be verified that the velocity profile generated by [1] is smoothed out.

5.4. **Four-Vortex Problem.** In this subsection, we consider the four-vortex problem [19]. The vorticity is given by the sum of four vortices in the unit square $\Omega = [0, 1] \times [0, 1]$. Each vortex is centered at $\{(x_i, y_i) \mid i = 1, \ldots, 4\} = \{(0.05,\ 0.05),\ (0.59, 0.5),\ (0.455, 0.5 + 0.45\sqrt{3}),\ (0.455, 0.5 - 0.45\sqrt{3})\}$ with strength $\eta_i = -150,\ 50,\ 50$ and 50 respectively. So the initial vorticity is given by

$$\omega = \sum_{i=1}^{4} \eta_i \frac{1}{2} \left(1 + \tanh(100(0.03 - r_i))\right),$$

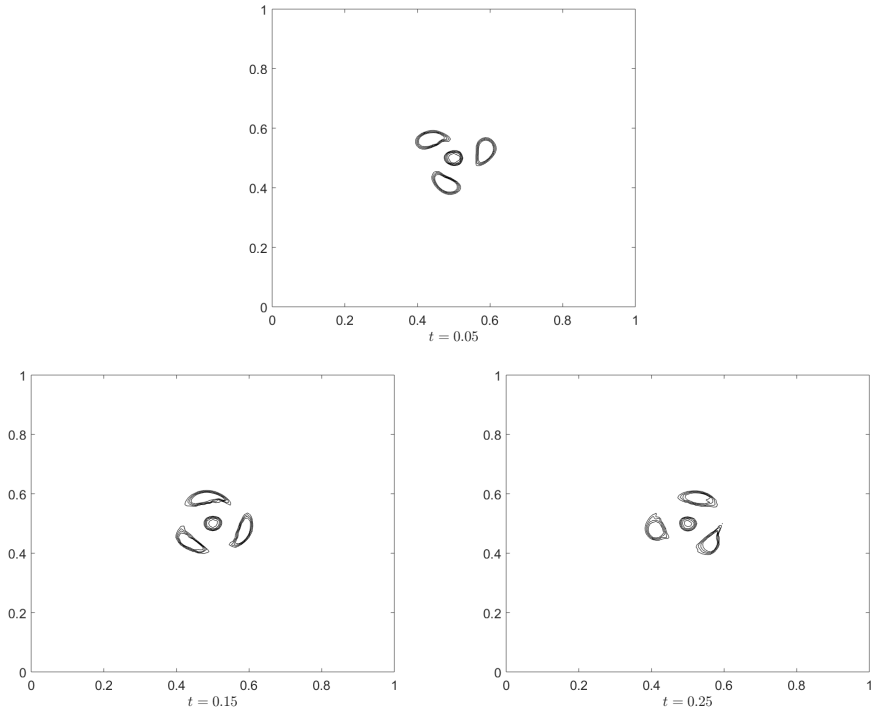

FIGURE 7. Contour plots of vorticity for the four-vortex on 128×128 grid at times $t = 0.05\ 0.15\ 0.25$.

where $r_i = \sqrt{(x - x_i)^2 + (y - y_i)^2}$. Then the initial velocity can be found from the steam function, which is the solution of the following Poisson equation

$$\begin{aligned} -\triangle\psi &= \omega \ \text{ in } \Omega, \\ \psi &= 0 \ \ \text{ on } \partial\Omega, \end{aligned}$$

and then projected onto the divergence-free vector field.

Since the initial velocity is generated by strong vortices in a small number of points, enforcing discrete energy stability to the numerical solution seems to be difficult. We demonstrate that the suggested method based on mathematical analysis does not depend on the complexity of the given problem. The sourcing term is not considered and the viscosity μ is set to be 0.0001. Figure 7 depicts the contour lines of the vorticity on 128×128 grid at $t = 0.05,\ 0.15,\ 0.25$, which agree with the one in [19]. In order to verify that Theorem 4.1 is valid for this problem, we note that the result of Theorem 4.1 can be seen as

$$\left\|E^{n+1}\right\|^2 = \|E^n\|^2 - \triangle t\mu||\nabla U^{n+\frac{1}{2}}||^2.$$

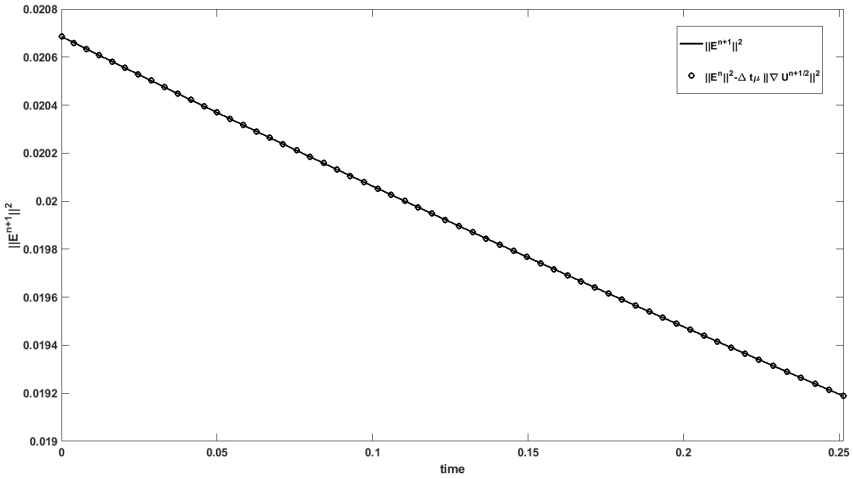

FIGURE 8. Comparison on $\left\|E^{n+1}\right\|^2$ and $\|E^n\|^2 - \triangle t\mu||\nabla U^{n+\frac{1}{2}}||^2$ of a four-vortex problem on 128×128 grid .

Figure 8 shows the profiles of $\left\|E^{n+1}\right\|^2$ and $\|E^n\|^2 - \triangle t\mu||\nabla U^{n+\frac{1}{2}}||^2$ at the same time for the above simulation. The result demonstrates that the result of Theorem 4.1 holds regardless of the complexity inherited in the problem.

6. CONCLUSION

In this study, we first reported that many standard explicit second-order methods fail to be strongly L^2 stable for solving a linear convection equation. We introduced an implicit finite difference method that is strongly L^2 stable and second-order accurate for solving the linear convection. The implicit method was then applied to solving the incompressible Navier-Stokes equations. As a result, we obtained a semi-implicit method that can solve the equations with the guaranteed stability and the second-order accuracy. All the numerical results validate the proposed stability and accuracy. The salt-and-pepper example is a nasty example that starts with a random velocity field, either 1 or 0, without a viscosity to damp out. Even with the hard example, our method showed the sharp preservation of energy. In our analysis, the integration-by-parts is essential to achieve the stability. For that purpose, we assumed domain to be rectangular and took the MAC space configuration that enables the integration-by-parts in discrete level. We acknowledge that the assumption on the domain is very restrictive, and hope to enhance the method to incorporate general domains in the near future. Though it is restrictive on the choice of domain, we expect that the method can be a very reliable tool, especially in real-time simulations, due to its guaranteed stability and second- order accuracy.

ACKNOWLEDGMENTS

The research of C. Min and Y.Park was supported by Basic Science Research Program through the National Re-search Foundation of Korea funded by the Ministry of Education (2017-006688 and 2019R1A6A1A11051177). The research of Byungjoon Lee was supported by NRF grant 2017R1C1B1008626 and POSCO Science Fellowship of POSCO TJ Park Foundation.

REFERENCES

[1] B. Lee and C. Min, "An energy-stable method for solving the incompressible navier-stokes equations with non-slip boundary condition," *Journal of Computational Physics*, vol. 360, pp. 104–119, 2018.
[2] A. W. J. Carlson, A.Jaffe, *The millennium prize problems*. American Mathematical Soc., 2006.
[3] G. Ansanay-Alex, F. Babik, J. Latché, and D. Vola, "An l2-stable approximation of the navier–stokes convection operator for low-order non-conforming finite elements," *International Journal for Numerical Methods in Fluids*, vol. 66, no. 5, pp. 555–580, 2011.
[4] R. Herbin and J.-C. Latché, "Kinetic energy control in the mac discretization of compressible navier-stokes equations," *International Journal on Finite Volumes*, vol. 7, no. 2, p. electronic, 2010.
[5] M. Gunzburger, N. Jiang, and Z. Wang, "A second-order time-stepping scheme for simulating ensembles of parameterized flow problems," *Computational Methods in Applied Mathematics*, 2017.
[6] A. Takhirov and J. Waters, "Ensemble algorithm for parametrized flow problems with energy stable open boundary conditions," *arXiv preprint arXiv:1808.09131*, 2018.
[7] G. M.Benzi and J.Liesen, "Numerical solution of saddle point problems," vol. 14, pp. 1–137, 2005.
[8] V. Girault and P.-A. Raviart, *Finite element methods for Navier-Stokes equations: theory and algorithms*, vol. 5. Springer Science & Business Media, 2012.
[9] R. Glowinski, T.-W. Pan, and J. Periaux, "A fictitious domain method for external incompressible viscous flow modeled by navier-stokes equations," *Computer Methods in Applied Mechanics and Engineering*, vol. 112, no. 1-4, pp. 133–148, 1994.
[10] A. J. Chorin, "A numerical method for solving incompressible viscous flow problems," *Journal of computational physics*, vol. 135, no. 2, pp. 118–125, 1997.
[11] J. Kim and P. Moin, "Application of a fractional-step method to incompressible Navier-Stokes equations," *J. Comput. Phys.*, vol. 59, pp. 308–323, 1985.
[12] J. B. Bell, P. Colella, and H. M. Glaz, "A second order projection method for the incompressible Navier-Stokes equations," *J. Comput. Phys*, vol. 85, pp. 257–283, 1989.
[13] D. B. R. C. M. Minion, "Accurate projection methods for the incompressible Navier-Stokes equations," *J. Comput. Phys.*, vol. 168, pp. 464–499, 2001.
[14] F. H. Harlow and J. E. Welch, "Numerical calculation of time-dependent viscous incompressible flow of fluid with a free surface," *Physics of Fluids*, vol. 8, no. 3, pp. 2182–2189, 1965.
[15] E. T. G.-S. Jiang, "Nonoscillatory central scheme for multidimensional hyperbolic conservation laws," *SIAM Journal of Scientific Compution*, vol. 19, no. 6, pp. 1892–1917, 1998.
[16] A. Harten, B. Enquist, S. Osher, and S. Chakravarthy, "Uniformly high-order accurate essentially non-oscillatory schemes III," *J. Comput. Phys.*, vol. 71, pp. 231–303, 1987.
[17] C.-W. Shu, *Essentially non-oscillatory and weighted essentially non-oscillatory schemes for hyperbolic conservation laws*, vol. 1697. Springer, 1998.
[18] A. Iserles, "A first course in the numerical analysis of differential equations," pp. 42–47, 2008.
[19] A. Almgren, J. Bell, P. Colella, L. Howell, and M. Welcome, "A conservative adaptive projection method for the variable density incompressible Navier-Stokes equations," *J. Comput. Phys.*, vol. 142, pp. 1–46, 1998.